EFDA–JET–PR(10)37

J. Svensson, O. Ford, D.C. McDonald, A. Meakins, A. Werner, M. Brix,
A. Boboc, M. Beurskens and JET EFDA contributors

Modelling of JET Diagnostics using Bayesian Graphical Models

Modelling of JET Diagnostics using Bayesian Graphical Models

J. Svensson[1], O. Ford[2], D.C. McDonald[3], A. Meakins[3], A. Werner[1], M. Brix[3], A. Boboc[3], M. Beurskens[3] and JET EFDA contributors*

JET-EFDA, Culham Science Centre, OX14 3DB, Abingdon, UK

[1]Max-Planck-Institut für Plasmaphysik, Teilinsitut Greifswald, EURATOM-Assoziation, D-17491, Greifswald, Germany
[2]Blackett Laboratory, Imperial College, London SW7 2BZ, UK
[3]EURATOM-CCFE Fusion Association, Culham Science Centre, OX14 3DB, Abingdon, OXON, UK
** See annex of F. Romanelli et al, "Overview of JET Results", (23rd IAEA Fusion Energy Conference, Daejon, Republic of Korea (2010)).*

Preprint of Paper to be submitted for publication in
Contributions to Plasma Physics

ABSTRACT.
Modern nuclear fusion experiments utilise a large number of sophisticated plasma diagnostics, which are sensitive to overlapping subsets of the physics parameters of interest. The mapping between the set of all physics parameters (the plasma 'state') and the raw observations of each diagnostic, will depend on the particular physics model used, and will also be inherently probabilistic. Uncertainty enters into the mapping between model parameters and observations through the inability of most models to predict the precise value of an observation, and also through aspects of the diagnostic itself, such as calibrations, instrument functions etc. To optimally utilise observations from multiple diagnostics and properly deal with all aspects of model uncertainties is very difficult with today's data analysis infrastructures. For this work, the Minerva analysis framework [1, 2] has been used, which implements a flexible and general way of modelling and carrying out analysis on this type of interconnected probabilistic systems by modelling of diagnostics, physics models and their dependencies through the use of Bayesian graphical models [3]. To date about 10 diagnostic systems have been modelled in this way at JET, which has already led to a number of new results, including the reconstruction of flux surface topology and q-profiles without an equilibrium assumption [4], profile inversions including uncertainty in the positions of flux surfaces, first experimental verification of relativistic effects to explain polarimetry measurements [5], and a substantial increase in accuracy of JET electron density and temperature profiles, including improved pedestal resolution, through the joint analysis of three different diagnostic systems [6].

1. INTRODUCTION

1.1 CHAINED ANALYSIS

Analysis of experimental data in large nuclear fusion experiments is currently done independently and differently for each diagnostic system. There is very limited infrastructure support for scientific analysis itself, with the effect that the substantial complexity of analysis of diagnostic data, testing of models, validation of results from different diagnostics etc, is a semi-manual, time consuming and non-transparent process, which, as will be explained further down, also limits the applicability of diagnostics for inference on physics models, and can substantially underutilise diagnostic data.

Typically, data analysis is done in chains of purpose-built diagnostic codes run after each experiment. The order in which the codes are executed, is determined by the dependencies each diagnostic code has on physics parameters estimated from codes run previously. This approach has some major shortcomings:

- The dependencies between diagnostic codes leads to unmanaged error propagation, e.g. ne or Te profiles from a Thomson scattering diagnostic is used further down the chain by another diagnostic code that estimates some other parameter from its measurements.
- Dependencies imply sensitivity to the same physics parameter. These could be utilised to extract more information about the underlying common parameter [7, 8, 4, 6]. Such dependencies can provide much information, but are not possible to explore within today's analysis infrastructure.

- Physics assumptions, parameterisations, smoothing assumptions etc., are spread out and hidden among the different analysis codes, usually rigidly frozen into compiled code. It is therefore a huge effort to assess what exactly the full scientific model behind the analysis of data from an experiment is, which has implications for the scientific standards of conclusions based on such models.

1.2 THE MINERVA FRAMEWORK

The Minerva framework [1, 2] tries to remedy these shortcomings by implementing a standardised scientific analysis infrastructure, where modelling of diagnostics, analysis of measurements, exchanging of underlying physics assumptions, and experimental design, are all done in a unified way. To accomplish this, Minerva uses the formal concept of Bayesian graphical models [3]. Being an amalgamation of probability theory and graph theory, it allows all functional and probabilistic dependencies between physics models and diagnostic raw data, diagnostic setup parameters etc, to be formally and explicitly defined (figure 1). The formal specification then represents a full scientific model for a given analysis scenario, and makes it possible to apply generic operations on the graph, such as different inversion methods, which are not tied a particular diagnostic. By using standard interfaces, multiple diagnostics can be combined, for joint inference on common physics parameters, thereby optimally utilising the diagnostic measurements. This can also be used to automatically calibrate diagnostics (see section 4), and can lead to a substantial increase in accuracy of inferred parameters.

The loose coupling and building block approach of Minerva also allows different assumptions behind the analysis of data from multiple diagnostics to be changed, such as assumptions on parameterisations and smoothness of profiles, and physics assumptions such as the Grad-Shafranov assumption (see section 3). Such assumptions determine how much information, and about what physics parameters, a diagnostic can contribute. Models implemented in Minerva are generative (figure 2), that is, measurements can be simulated from underlying physics assumptions and diagnostic setup parameters, such as line of sight geometries, calibrations etc. Thus, the same system used for analysis can also be used for experimental design.

The generic description and implementation of diagnostics and physics models in Minerva makes it possible to transfer diagnostic models to other machines [9]. The framework is currently used at the JET, MAST, H1 and W7-X experiments. We will here show some results from the application of such models at JET. The mathematical underpinning of Minerva, Bayesian probability and Bayesian graphical models, are introduced in section 2. Section 3 describes the modelling of the JET magnetics, flux surfaces and equilibrium. In section 4 a joint analysis of JET's two LIDAR systems with an 8-channel interferometer system is presented. Section 5 gives a summary and outlook.

2. BAYESIAN PROBABILITY AND GRAPHICAL MODELS

If we define the physics state S as the values of all free parameters and nuisance parameter in a

given model, we get for the probability distribution over S, from Bayes formula

$$p(S|D) = \frac{p(S|D)\ p(S)}{p(D)} \tag{1}$$

where D is the observed data. p(S), the prior distribution, expresses our knowledge about the state S before any observations are made. This is used to express regularization assumptions, smoothing assumptions, or physics constraints on the free parameters of the model. It is largely this entity that makes it possible to move this type of "soft" or auxiliary assumptions from the analysis algorithm to the model itself. p(D|S), the likelihood, describes the distribution of observations that are expected for a given physics state S. From these two distributions the posterior distribution, p(S|D) can be calculated up to a normalisation constant p(D) that is independent of the state S.

To infer the posterior of S from observations from a number of diagnostics simultaneously, we use the fact that the observations from different diagnostics are conditionally independent given the common physics state S:

$$p(S|\{D_i\}) = \frac{p(S|D)\prod_{i=1}^{N} p(D_i|S)}{p(\{D_i\})} \tag{2}$$

This simple formula hides a substantial complexity: the likelihoods for the different diagnostic observations, $p(D_i|S)$, include the full mapping between the physics state S, including physics model, diagnostic nuisance parameters such as calibration factors, stray light, line of sight geometry etc, and the expected observation of that diagnostic. It is the assumptions in this likelihood, the choice of parameters in S, and the form of the prior distribution, that form our scientific model. An elegant and transparent way of unfolding and handling this type of complex probabilistic models is by expressing them in terms of Bayesian graphical models (figure 1), where each node represents a deterministic function, or a probability distribution conditioned on its parents. By associating nodes (a, b, c, n, d1, d2 in figure 1) with specific conditional probability distributions, the joint distribution of observations and free parameters, which is proportional to the posterior distribution, can be formed automatically from the graph definition, and so need not be hardcoded into legacy codes. Inversion methods, such as nonlinear optimisation of the free parameters to find a maximum probable state (MAximum Posterior (MAP)), or sampling methods such as Markov Chain Monte Carlo (MCMC) can then be applied to the graph.

3. MAGNETIC MODEL

A fundamental quantity to infer, important for much diagnostic analysis, is the magnetic field structure. We we will here describe two Minerva models for the magnetic field, the first using a magnetostatic assumption, and the second a force balance assumption. Inference on the internal magnetic field from diagnostic measurements involves modelling of the plasma current distribution, poloidal and toroidal field coils, and in some cases passive structures, such as iron core or vessel

eddy currents. For the toroidal current distribution model, we here use a grid of solid current beams [4] (figure 3), and the magnetization of the JET iron core is treated as a nuisance contribution to the field inside the plasma. From this model, the marginal posterior over current beams can be calculated, and by picking samples from the posterior current distribution, and calculating flux surfaces, magnetic axis position, x-point etc from those samples, uncertainties on those quantities can be established. Prior regularizing assumptions specify the necessary assumptions on the scale lengths of the toroidal current distribution, from which the posterior current distribution can be calculated using different sets of diagnostics. Figure 4 shows samples of posterior flux surfaces from graphical models including increasingly more diagnostics connected to the toroidal current model. In figure 4c six diagnostic systems are used jointly to infer the flux surface topology, without using any specific equilibrium assumption, and so will not be sensitive to possible anisotropic pressure, plasma rotation etc.

We can now use the information about the uncertainty of the flux surface coordinate system in the analysis of other diagnostic data. Figure 5 shows ne profiles inversed using JET interferometer data, from maximum likely flux surfaces (figure 5a), and taking into account the uncertainty in the flux surfaces through repeated interferometry inversions on samples from the posterior flux using diagnostic coils and the MSE diagnostic (figure 2). As can be seen in the figures, the central dip of the density profile can be explained by uncertainty in the flux coordinates themselves.

We can now use the same diagnostic models, and change the physics model to include a force balance assumptions as well. A Grad-Shafranov constraint is added to the graph model by adding a poloidal current model, pressure model, and constraint nodes that impose a given prior assumption on the difference between the toroidal current distribution as modelled above, and the right hand side of the Grad-Shafranov equation (figure 6b):

$$Rp' + \frac{\mu_0}{R} ff' \tag{3}$$

where R is the major radius, p' the pressure derivative with respect to normalised poloidal flux, and f the poloidal current flux.

With such a constraint, the toroidal current distribution can be inferred on a high resolution beam grid using only external magnetic diagnostics (JET pickup coils, saddle coils and flux loops), including unexpectedly high detail of local features, especially at the plasma edge (figure 6) [10]. Work is currently ongoing to explore the posterior current uncertainties using Markov Chain Monte Carlo sampling.

4. COMBINED CORE LIDAR, EDGE LIDAR AND INTERFEROMETRY

Another example of how a modular framework can benefit analysis is a the following detailed Minerva models for the JET core and edge LIDAR systems [6], the combination of which with the interferometer system previously mentioned, gives a substantial increase in accuracy of n_e and T_e

profiles, and manages to resolve the pedestal region to an extent not possible with any diagnostic used alone. Figure 7 shows inferred n_e and T_e profiles from this combined system. For this model, the position and absolute density calibrations of both LIDAR systems, and the absolute temperature calibration of the edge LIDAR have been free parameters, the combined information of these three systems being enough to infer both ne and Te profiles to the accuracy indicated in figure 6. This shows that this approach can also lead to powerful selfcalibrating systems in some cases.

SUMMARY

Modelling the complex inference systems in nuclear fusion experiments with Bayesian graphical models as implemented in the Minerva framework, makes it possible to have full control over all assumptions behind a scientific model, easily change physics assumptions, and combine different diagnostics for more accurate inference on the physics parameters of interest. The intrinsic Bayesian approach allows full exploration of the influence of all uncertainties in the combined model. This modular Bayesian graph approach could potentially be used for very large sets of diagnostics, providing a generic data analysis framework for nuclear fusion experiments that would be able to optimally utilise all information in the system.

ACKNOWLEDGEMENTS

This work was supported by EURATOM and carried out within the framework of the European Fusion Development Agreement. The views and opinions expressed herein do not necessarily reflect those of the European Commission.

REFERENCES

[1]. J. Svensson, A. Werner, Large Scale Bayesian Data Analysis for Nuclear Fusion Experiments, Proceedings IEEE Workshop on Intelligent Signal Processing WISP 2007

[2]. http://www.seed-escience.org

[3]. J. Pearl, Probabilistic Reasoning in Intelligent Systems: Networks of Plausible Inference, Morgan Kaufmann Publishers, 1988

[4]. J. Svensson, A. Werner, Current Tomography for Axisymmetric Plasmas, Plasma Physics and Controlled Fusion **50** No 8 (August 2008)

[5]. O. Ford, J. Svensson, A. Boboc, D.C. McDonald, Experimental verification of relativistic finite temperature polarimetry effects at JET, Plasma Phys Control Fusion, **51**,No 6 (2009)

[6]. O Ford, J. Svensson, M. Beurskens, A. Boboc, J. Flanagan, M. Kempenaars, D.C. McDonald, Bayesian Combined Analysis of JET LIDAR, Edge LIDAR and Interferometry Diagnostics, EPS 2009, Sofia

[7]. R. Fischer, A. Dinklage, E. Pasch, Bayesian Modelling of Fusion Diagnostics, PPCF, 2003

[8]. J. Svensson, A. Dinklage, R. Fischer, J. Geiger, A. Werner, Integrating Diagnostic Data Analysis for W7-AS using Bayesian Graphical Models.", Review of Scientific Instruments, **75** p. 4219-4221, 2004

[9]. M.J. Hole, G. von Nessi, J. Bertram, J. Svensson, L.C. Appel, B.D. Blackwell, R.L. Dewar, and J. Howard, Model Data Fusion: developing Bayesian inversion to constrain equilibrium and mode structure, Journal of Plasma and Fusion Research, **9** (2010)

[10]. O. Ford, Tokamak Plasma Analysis Through Bayesian Diagnostic Modelling, PhD thesis, Imperial College, London.

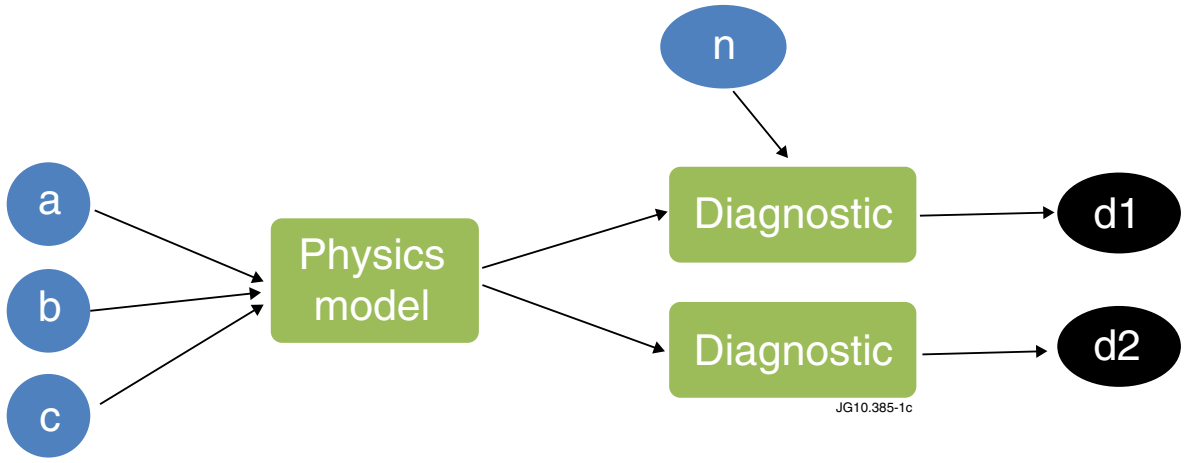

Figure 1. Schematic Minerva Bayesian graphical model for two diagnostics giving joint evidence on the same physics model. Ovals are probabilistic nodes, of which a,b,c are free parameters of the physics model, n is a nuisance parameter of a diagnostic, and d1, d2 observations. In reality, also the physics and diagnostic models are implemented as exchangeable subgraphs. Inversion of this graph would make both d1 and d2 contribute towards inferring a,b and c. The nuisance parameter n would be marginalised out.

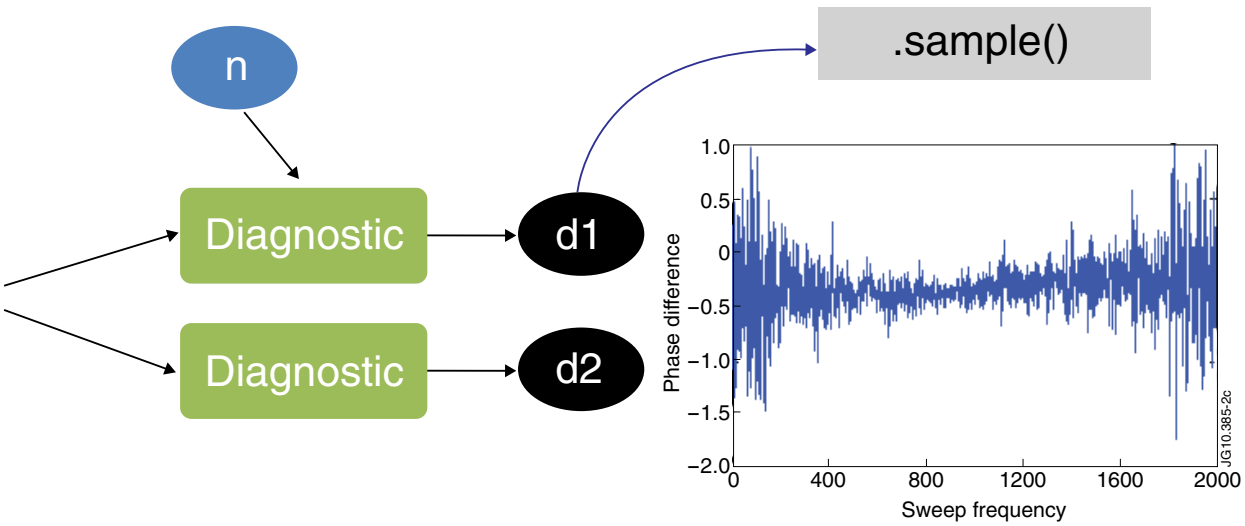

Figure 2. All Minerva models are generative, so each observation can be sampled/simulated conditioned on the set of dependent parameters that are ancestors of the observation nodes.

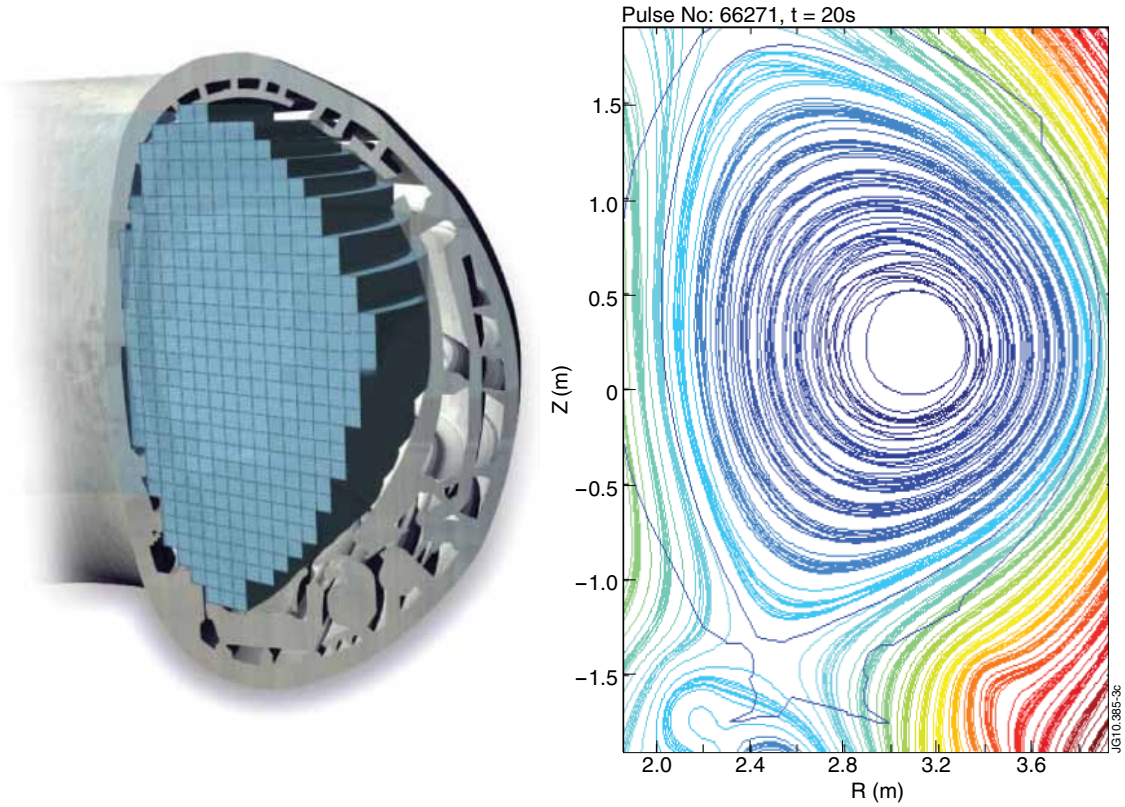

Figure 3. a) Model of the toroidal current distribution as a grid of solid current beams. b) samples of flux surfaces from posterior [4].

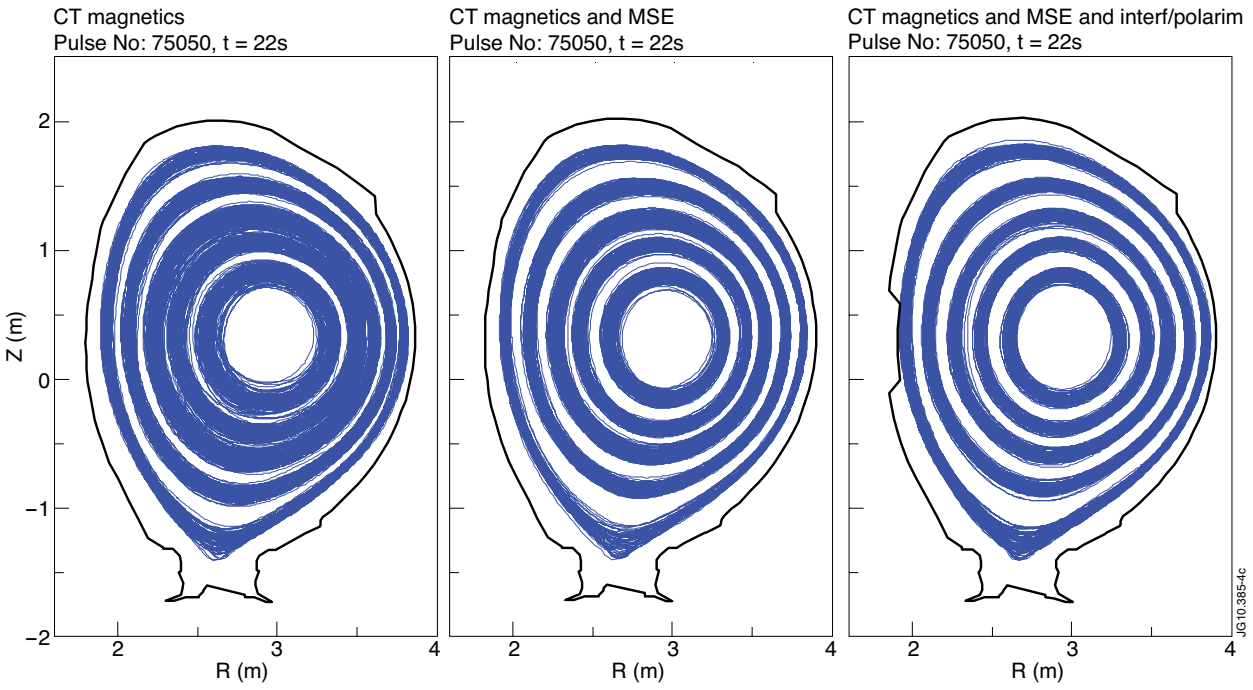

Figure 4. Samples from posterior of flux surfaces for different sets of diagnostics for the same prior. Width of a flux surface corresponds to the uncertainty of the flux surface. From left to right: a) Pickup coils, saddle coils and flux loops, b) additional Motional Stark (MSE) measurements, c) additional polarimetry and interferometry measurements.

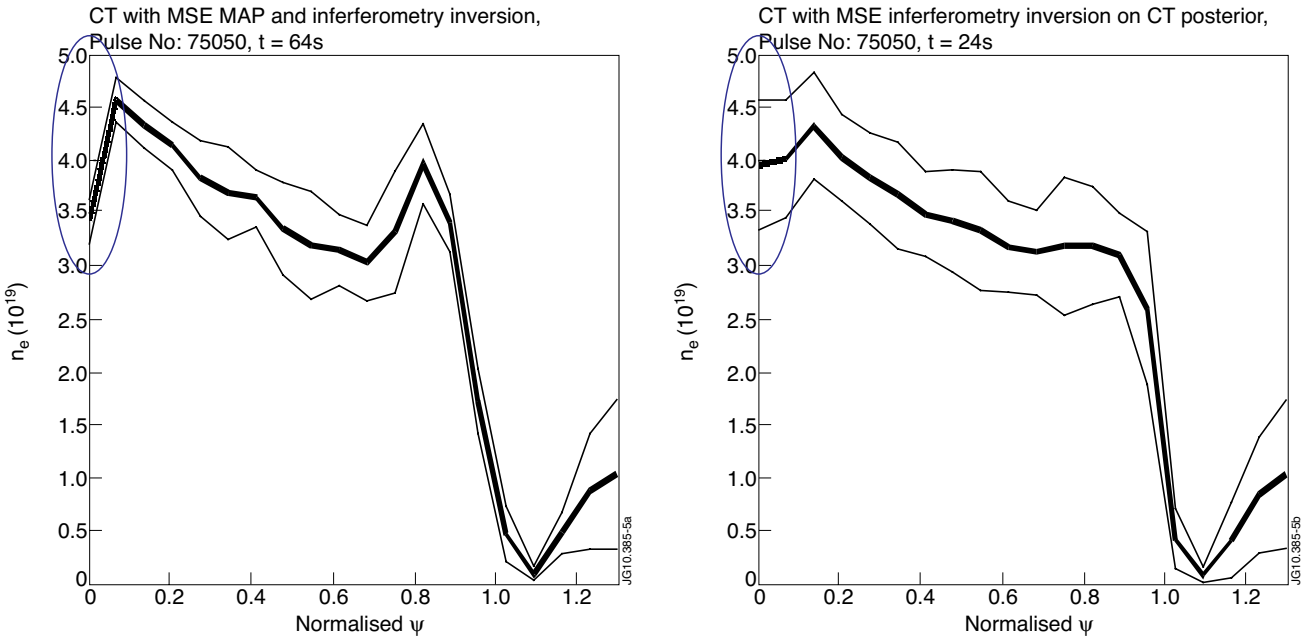

Figure 5. Inversion of the JET 8 channel interferometry signals from a) Maximum probable flux surface topology, and b) On repeated samples from the posterior of the flux surfaces, showing that the uncertainty in the mapping itself can explain the hollow profiles in a). JET Pulse No: 75050, t = 24s.

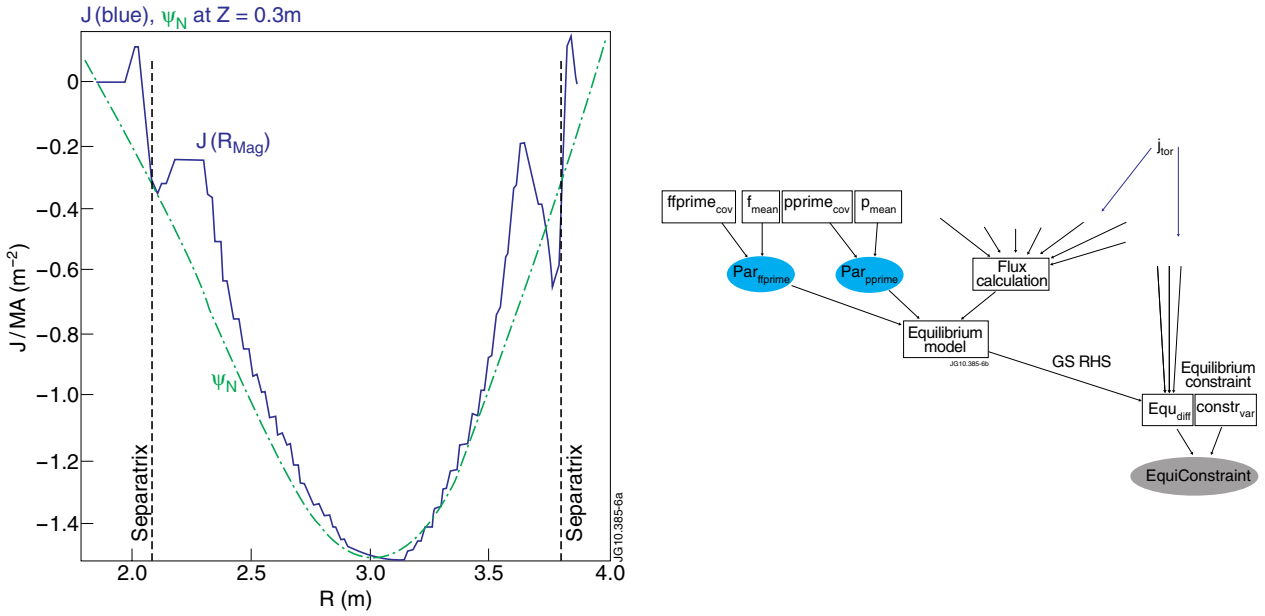

Figure 6. MAP inference on the toroidal current distribution (left) by adding a Grad- Shafranov constraint in a Minerva graphical model (right).

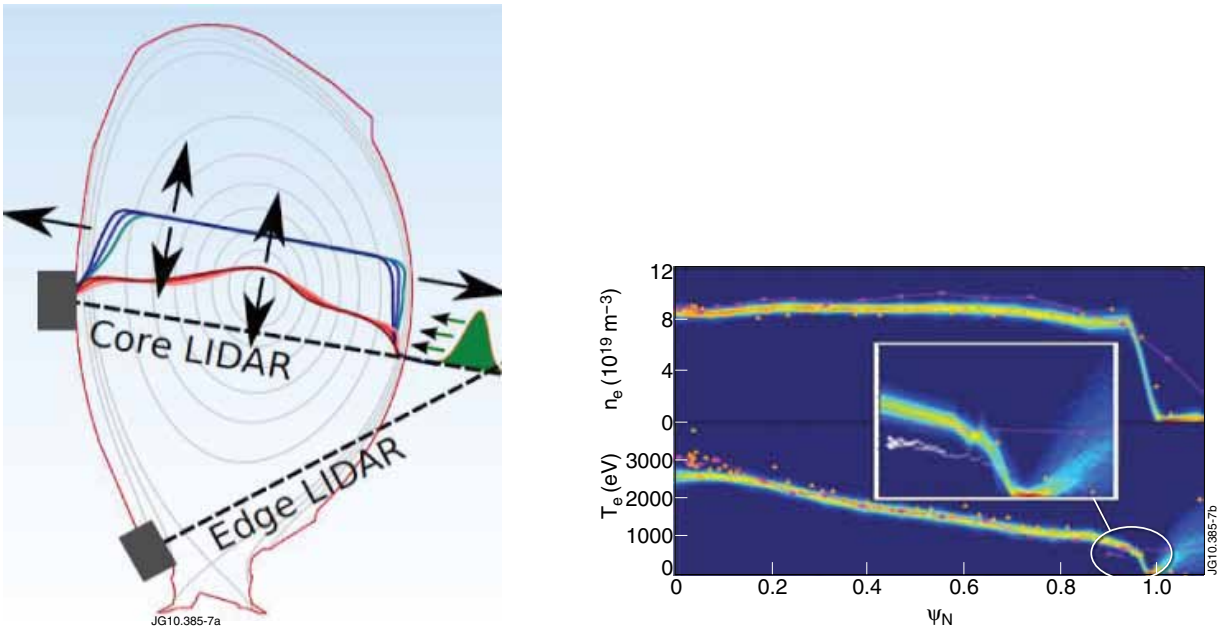

Figure 7. a) Laser beamline for the two JET LIDAR systems. b) ne and Te profiles. Colored bands are marginal posterior density, violet is standard core LIDAR analysis, white edge LIDAR stand-alone analysis, orange are independent high resolution Thomson scattering measurements.